# Chemical Vapor Deposition of Graphene on a "Peeled-Off" Epitaxial Cu(111) Foil: A Simple Approach to Improved Properties

Hak Ki Yu,[†,‡] Kannan Balasubramanian,[§] Kisoo Kim,[⊥] Jong-Lam Lee,[⊥] Manisankar Maiti,[∥] Claus Ropers,[∥] Janina Krieg,[§,#] Klaus Kern,[§] and Alec M. Wodtke[†,‡,*]

[†]Institute for Physical Chemistry, University of Göttingen, 37077 Göttingen, Germany, [‡]Max Planck Institute for Biophysical Chemistry, 37077 Göttingen, Germany, [§]Max Planck Institute for Solid State Research, 70569 Stuttgart, Germany, [⊥]Department of Materials Science and Engineering and Division of Advanced Materials Science, Pohang University of Science and Technology (POSTECH), 790-784 Pohang, Korea, and [∥]IV. Physical Institute, University of Göttingen, 37077 Göttingen, Germany. [#]Present address: GSI Helmholtz Center for Heavy Ion Research, 64291 Darmstadt, Germany.

**ABSTRACT** We present a simple approach to improving the quality of CVD grown graphene, exploiting a Cu(111) foil catalyst. The catalyst is epitaxially grown by evaporation on a single crystal sapphire substrate, thickened by electroplating, and peeled off. The exposed surface is atomically flat, easily reduced, and exclusively of (111) orientation. Graphene grown on this catalyst under atmospheric CVD conditions and without wet chemical prereduction produces single crystal domain sizes of several hundred micrometers in samples that are many centimeters in size. The graphene produced in this way can easily be transferred to other substrates using well-established techniques. We report mobilities extracted using field-effect (as high as 29 000 $cm^2 V^{-1} s^{-1}$) and Hall bar measurement (up to 10 100 $cm^2 V^{-1} s^{-1}$).

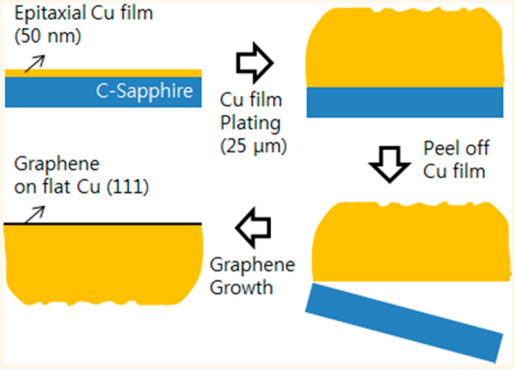


**KEYWORDS:** chemical vapor deposition · copper catalyst · graphene · epitaxial Cu (111) foil · peel-off · carrier mobility

Graphene is commonly synthesized by chemical vapor deposition (CVD) on copper (Cu) foils, a method favored for large-scale production.[1−5] Unfortunately, the physical properties of graphene produced in this way typically do not reach those of exfoliated graphene. CVD graphene typically exhibits a high density of crystalline defects associated with grain boundaries as well as chemical impurities or defects. These defects result from surface chemical interactions with the polycrystalline Cu catalyst occurring during the CVD process. Problems associated with present Cu foil catalysts include the following: poly crystallinity of the catalyst surface (the (111) surface is most desirable for graphene CVD[6−8]), multiple domain formation during CVD, surface roughness as well as chemical impurity arising from copper oxidation.[9−11]

Graphene grown on an epitaxial Cu(111) film has been reported by several groups in attempts to produce samples with higher carrier mobility.[7,12−14] Here, a mother substrate of C-plane sapphire is used to produce an epitaxial Cu film, typically ∼200 nm in thickness, and the graphene is grown on top of the copper. The surface of such epitaxially grown Cu(111) films is not atomically flat. Because it is so thin, it is also fragile; for example, the removal of the copper from the sapphire/copper/graphene sandwich structure is difficult. The catalytic surface is also exposed, making it vulnerable to uncontrolled oxidation. Up to now, this approach has resulted in graphene properties with best carrier mobility of 2500 $cm^2 V^{-1} s^{-1}$.[13]

We have found a simple way to prepare an epitaxial copper foil on C-plane sapphire such that it can be subsequently peeled away. The peeling process exposes a fully intact Cu(111) crystalline surface, which is chemically clean and atomically flat. The sapphire substrate can be reused;

* Address correspondence to alec.wodtke@mpibpc.mpg.de.

Received for review June 26, 2014 and accepted July 24, 2014.

**Published online July 24, 2014**
10.1021/nn503476j

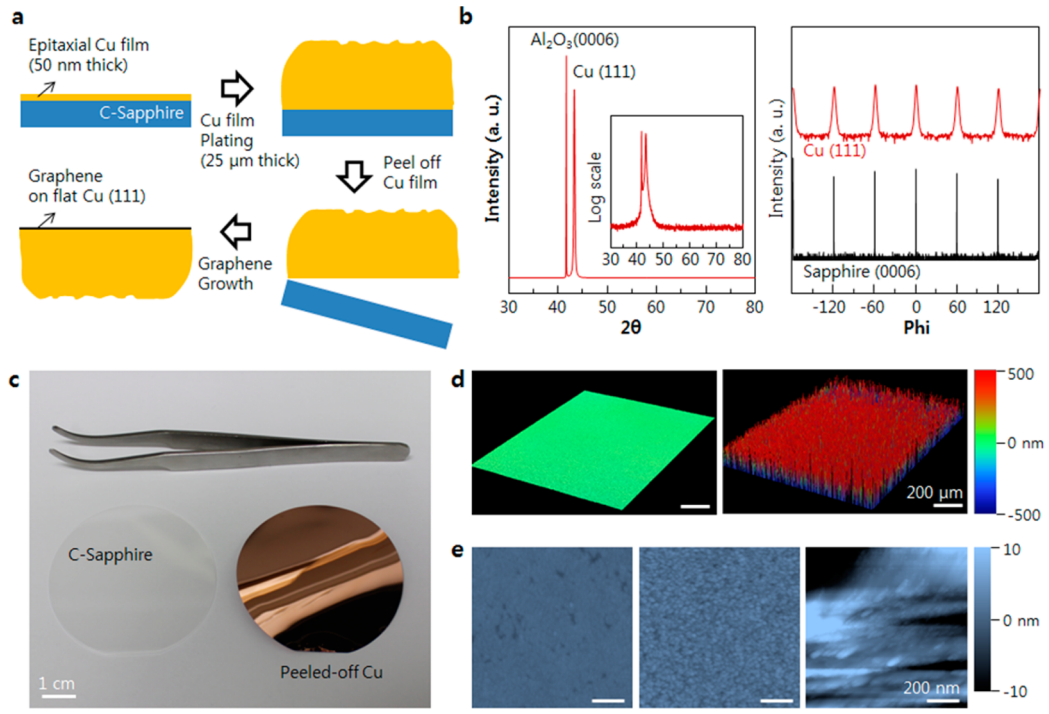


**Figure 1. Method for preparing peeled-off Cu foil and its structural properties. (a) Schematic of the fabrication procedure for peeled-off Cu foil and its use in CVD graphene synthesis. (b) X-ray diffraction of the epitaxial Cu(111) film (50 nm thickness) while it is still adhered to the C-plane (0006) sapphire, first step of panel a. The absolute angles seen in the 2$\theta$ scan are consistent with the characteristic lattice constants of $Al_2O_3$ (0006) and Cu(111). The phi-scan (azimuthal scan) analysis is carried out with $\theta$ fixed along the Cu $\{2\bar{2}0\}$ direction (red curve) and along the sapphire $\{3\bar{3}00\}$ (black curve). Both exhibit coherent peaks spaced by 60°, characteristic of their epitaxial spatial relationship: $(111)[1\bar{1}0_{Cu}] \parallel (0001)[1\bar{1}00]_{C\text{-}sapph}$. (c) Digital camera image of Cu(111) foil catalyst peeled-off from a 2-in. C-plane sapphire. Scale bar, 1 cm. (d) Surface roughness analysis of peeled-off Cu foil—peel-off exposed surface (left) and opposite Cu surface after electrochemical thickening (right), measured by a 3D-profiler with 20 nm resolution. Scale bar, 200 $\mu$m. (e) Surface roughness measured by AFM. Scale bar, 200 nm; peel-off exposed surface (left), opposite surface before electrochemical thickening (middle), and opposite surface after electrochemical thickening (right).**

our approach effectively offers a practical means of fabricating (111) single crystalline catalyst surfaces for graphene growth. The graphene grown with this catalyst exhibits superior carrier mobility: up to 29 000 $cm^2 V^{-1} s^{-1}$ measured by the field effect method and up to 10 100 $cm^2 V^{-1} s^{-1}$ measured by the Hall bar method. Graphene domain sizes are typically several hundreds of $\mu$m and are stitched together in a continuous sample many cm's in size. The resulting graphene layers can easily be transferred to other substrates using well-established polymer coating and Cu etching techniques. The approach can be scaled to produce improved quality graphene sheets with several tens of centimeters in diameter.[15−17]

## RESULTS AND DISCUSSION

Figure 1a is a schematic illustration of the steps in the fabrication of graphene used in this work. First, an epitaxial Cu(111) film is grown on C-plane sapphire by evaporation to a thickness of several tens of nanometers. Subsequently, the film is thickened to several tens of micrometers by electrochemical means, at which point it is easily peeled away from the sapphire substrate. The side of the foil originally in contact with the sapphire is then used in catalytic CVD graphene growth similar to previous reports.

C-plane sapphire is an excellent choice as mother substrate since (i) it has a suitable (8.6%) lattice mismatch with Cu(111), sufficiently close to the Cu(111) lattice to allow epitaxial growth and sufficiently different to provide needed stress for ease in peel-off; (ii) it is a near perfect insulator and therefore compatible with electrochemistry; (iii) it has excellent and manipulable interface properties, which leads to easy peel-off of the metallic Cu;[18] (iv) it has a relatively low cost; and (v) it can be produced in sizes up to 15 in.[15−17] Furthermore, the mother substrate can be continuously reused.

The 50 nm thick epitaxial Cu film formed on C-plane sapphire shows exclusive (111) orientation prior to peel-off—see X-ray diffraction data in Figure 1b. The Cu—Cu distance between surface atoms in copper (111) is 0.255 nm, while the O—O surface atom distance in C-plane sapphire is 0.279 nm. The (8.6%) atomic spacing mismatch allows for pseudoepitaxial grown of Cu(111) on C-plane sapphire. We attribute the 6-fold azimuthal symmetry seen in X-ray diffraction to symmetry breaking of the 3-fold (111) surface pattern associated with fcc Cu when epitaxially grown on C-plane sapphire; the Moiré pattern of the interface has a 6-fold symmetry, even though both interfaces have 3-fold symmetry. See Supporting Information Figure S1.[19,20]

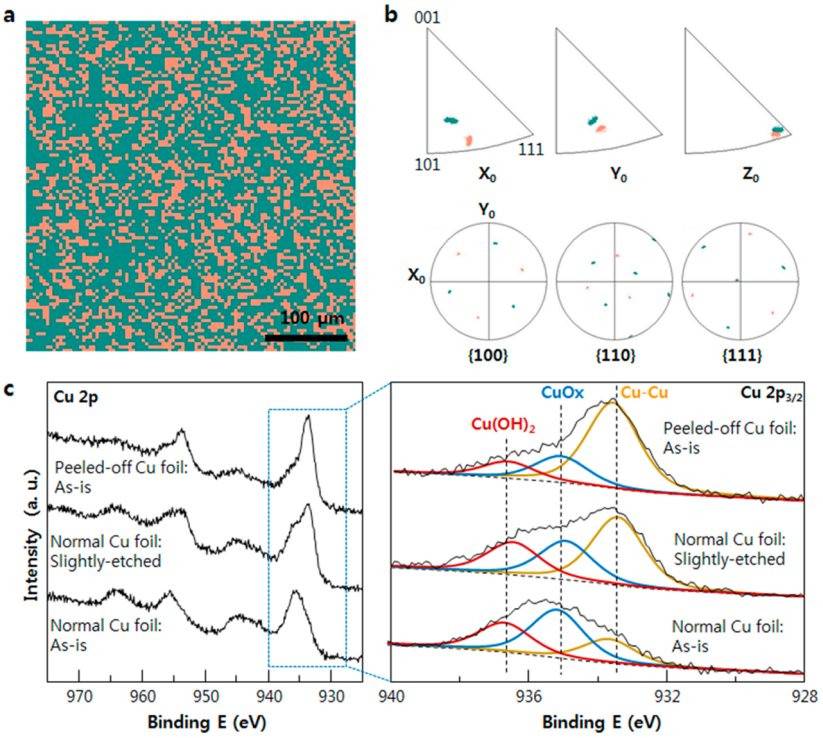


**Figure 2. Structural and chemical properties of peeled-off Cu(111) foil. (a) Electron backscatter diffraction (EBSD) map of peeled-off Cu(111) foil. The "EBSD map" clearly shows two interface derived diffraction patterns, indicated as orange and green (see also Supporting Information Figure S2). (b) Inverse pole figures and corrected pole figures of peeled-off Cu foil obtained by EBSD. The two diffractions (indicated as orange and green color) result from two different azimuthal orientations of the surface Cu(111). (c) X-ray photoemission spectra of several Cu foils. The fitting of Cu $2p_{3/2}$ was done based on ref 22. The peeled-off Cu(111) film catalyst is only modestly oxidized even after 1 week in ambient air. It is exclusively of (111) surface orientation.**

The compressive stress between the Cu film and C-plane sapphire combined with the weak adhesion between the two materials allows the Cu film to be peeled from the substrate easily (Figure 1c).

The side of the Cu foil that has been peeled away from the sapphire is exceedingly flat. Figure 1d shows flatness over a wide area as measured by a surface profiler with 20 nm resolution. The roughness of the peeled-off surface cannot be seen with this method even over the 1 mm area shown. By contrast, the opposite surface of the film electrochemically thickened and peeled off, shows a RMS roughness of 740 nm. Figure 1e shows higher resolution roughness measurements using air AFM over a smaller (1 $\mu$m square) area. The peeled-off Cu surface exhibits an RMS roughness of 0.40 nm. For comparison, the surface roughness of the opposing surface exhibits an RMS roughness of 0.86 nm before electrochemical thickening and 7.1 nm after.

We observed no damage to the Cu crystalline structure after peel-off, using electron backscatter diffraction (EBSD); however, two azimuthal orientation domains are formed. Figure 2a,b shows EBSD results revealing two kinds of 3-fold symmetric domains, indicated as orange and green (see also Supporting Information Figure S2). The two diffractions result from different azimuthal orientations of the Cu(111) surface. This may be due to an epitaxial twinning at the copper-sapphire interface, possibly resulting from peel-off. We estimate the size of the azimuthal surface domains shown in Figure 2a to be ~23 $\mu$m for the orange area and ~122.7 $\mu$m for the green area although this not much larger than the spatial resolution limit of our EBSD instrument.

The oxidation of Cu surfaces, forming CuO, $Cu_2O$, and $Cu(OH)_2$, is hard to avoid under ambient conditions since copper oxides are thermodynamically favored.[21] CVD using conventional copper foil catalysts normally involves removal of the native oxide prior to graphene growth, for examplem by treatment with acetic acid[21] or $(NH_4)_2S_2O_8$. By contrast, the peeled-off catalyst surface is formed in a chemically pure state and only begins to oxidize slowly upon exposure to air. Figure 2c shows X-ray photoemission spectra (XPS) in the Cu 2p region[22] for several Cu foil surfaces. Ordinary Cu foil yields a strong oxide signal in XPS compared to signals reflecting Cu−Cu bonding. By contrast, the peeled-off surface, stored in air for 1 week prior to analysis, shows only limited oxide formation. When the conventional copper foil is treated with $(NH_4)_2S_2O_8$ solution for 1 min, XPS still shows substantially more oxide compared to the untreated peeled-off Cu foil. See also the O 1s spectra in Supporting Information Figure S3.

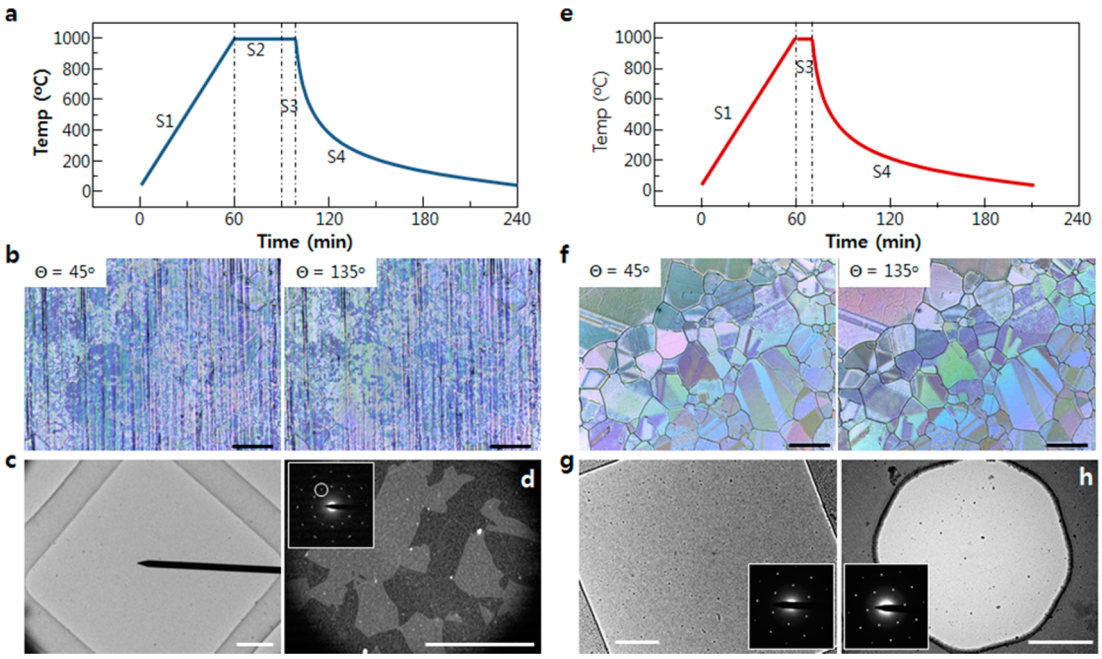


**Figure 3. Graphene synthesis on Cu foil. (a and e) CVD process for graphene growth on normal Cu foil (a) and peeled-off Cu foil (e). Neither wet chemical reduction nor high temperature annealing in hydrogen is needed for the peeled-off catalyst. (b and f) Polarized optical microscope images of liquid crystals spin-coated onto the graphene on normal Cu foil (b) and peeled-off Cu foil (f). Scale bar, 100 $\mu$m. Two polarization angles reveal ~100 um size graphene domains produced with the peeled-off catalyst. (c) TEM image of reference graphene after transfer to Quanti-foil-TEM grid (7 $\mu$m hole with 2 $\mu$m space). Scale bar, 1 $\mu$m. (d) Dark field TEM image of reference graphene. Inset shows selected area electron diffraction (SAED) and the diffraction spot used for dark field imaging. Scale bar, 500 nm. (g and h) TEM image of graphene grown from peeled-off Cu foil after transfer to Quanti-foil-TEM grids. Scale bar, 1 $\mu$m. Each inset shows the SAED.**

We now turn to a discussion of the graphene produced with the peeled-off catalyst. For comparison, we also prepared graphene on normal Cu foil (Alfa Aesar, item No. 13382, 99.8% purity) according to literature protocols[1] and on thin epitaxial films (See Supporting Information discussing Figure S4). The normal Cu foil required us to follow the temperature−time curve shown in Figure 3a, which included a substantial preannealing time of the Cu foil in a hydrogen reducing atmosphere at 1000 °C (step S2). Reductive annealing is essential to the success of CVD graphene growth using normal copper foil, both to remove residual oxide and to help form larger (111) crystalline domains. Even with reductive annealing, some copper oxides remain on the catalyst; these were identified as segregated $CuO_x$ nanoparticles by area resolved energy dispersed X-ray spectroscopy (EDX). See Supporting Information Figure S5a. These copper oxide nanoparticles degrade the quality of the CVD graphene and complicate transfer and removal. Wet chemical reduction methods have been employed to help ameliorate this well-known problem; for example, pretreatment in acetic[21] or hydrochloric acid[23] (see Supporting Information Figure S5b). Alternatively, electromechanical polishing to remove oxide has been reported.[24,25] We found that etching with $(NH_4)_2S_2O_8$ gave better results than any of these other methods. We etched normal Cu foil for the reference graphene growth by dipping in $(NH_4)_2S_2O_8$ solution for 1 min before CVD growth. This led to the best removal of Cu oxide nanoparticles (Supporting Information Figure S6) and the highest quality reference graphene.

Graphene films were synthesized from peeled-off epitaxial Cu(111) foil using the CVD method with methane as the carbon source and hydrogen as carrier gas. No wet chemical reduction or high temperature reductive preannealing was employed with this catalyst. Instead, the simplest possible temperature−time curve was used; see Figure 3e.

The graphene from the peeled-off catalyst exhibits higher crystalline quality than that produced on normal Cu foil. The domain size distribution can be probed by coating the graphene with a nematic liquid crystal (4-pentyl-4′-cyanobiphenyl (5CB)) and examining the sample with polarized optical microscopy.[26] These images are shown in Figure 3b (for normal foil catalyst) and Figure 3f (for peeled-off catalyst). By rotating the polarizer in the optical microscope by 90°, we visualize the domain size of the graphene samples.[26] For reference graphene, it is difficult to identify grain boundaries (Figure 3b), indicating that the grain size is close to the optical diffraction limit. By contrast, graphene from the peeled-off catalyst shows distinct grain boundaries for the copper catalyst (dark solid lines), as well distinct graphene domains, which are sensitive to the polarization angle. EBSD analysis of the peeled off catalyst after CVD growth still shows large (111) domains; however, the rotational orientation of the

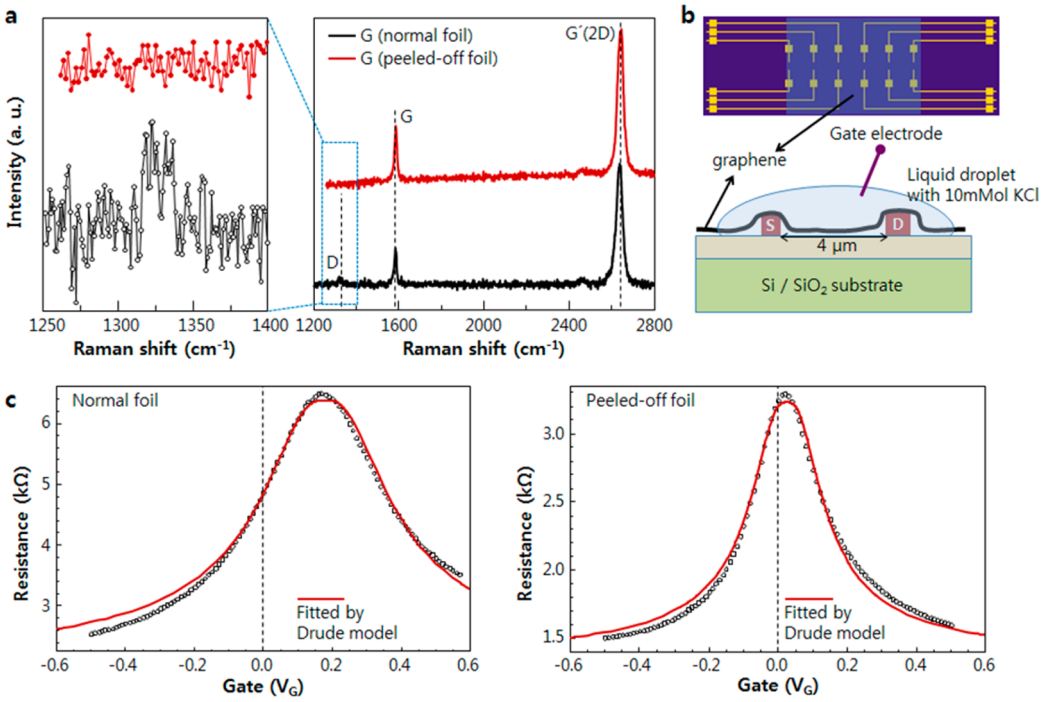


**Figure 4. Raman and transport properties of graphene. (a) Raman spectra of graphene with enlargement near the D band area. (b) Schematic of a graphene device for the field effect charge carrier mobility measurement. (c) The resistance of graphene measured across Source (S) and Drain (D) as a function of gate voltage, $V_G$. Dots represent data, while the continuous red line is obtained from the fitted Drude model. The Drude model fit to this data suggests that the charge carrier mobility of peeled-off graphene was as high as 29 000 $cm^2 V^{-1} s^{-1}$.**

domains is now more widely distributed (see Supporting Information Figure S7). The graphene domain-size is as large as 100 $\mu$m (Figure 3f). The small grain size of the reference graphene is confirmed by transmission electron microscopy (Figures 3c,d). Here, an area with 1 $\mu$m diameter is analyzed. The electron diffraction pattern shows 12 spots, indicating two crystalline orientations within the field of view. The dark-field image (Figure 3d) derived from the circled region in the inset of Figure 3d shows that the domain size is on the order of 0.5 $\mu$m or less, consistent with our polarimetry results. 6-fold symmetric electron diffraction patterns are obtained for graphene produced on peeled-off Cu foil (Figure 3g,h insets). The diffraction spots of several areas reveal no grain boundaries on the 1 $\mu$m length scale, a result also consistent with our polarimetry.

We conclude that the domain size of graphene obtained from a peeled-off catalyst is about 2 orders of magnitude larger than that obtained from a normal copper foil. It is likely that the large graphene domain size obtained from peeled-off catalyst reflects a smaller density of nucleation sites for graphene crystal growth on this nearly ideal copper catalyst.[27] This suggests that further improvements in catalyst preparation might lead to yet larger average domain sizes, a topic of ongoing effort in our laboratory.

Figure 4a shows Raman spectra of both peeled-off and reference graphene. The Raman spectrum shows typical features associated with monolayer graphene for both samples, namely an intensity ratio of the 2D and G lines between 2 and 3 as well as a symmetric 2D band with a fwhm of 36.0 $cm^{-1}$ for reference graphene and 32.6 $cm^{-1}$ for graphene from peeled-off Cu foil.[28] Moreover, the graphene grown on peeled-off Cu foil has no detectable D band. By contrast, we observe a weak D band for reference graphene.

We measured charge carrier mobilities of the graphene devices in liquid using field-effect and Hall bar configurations. The graphene sheets are transferred onto $Si/SiO_2$ chips with prepatterned electrodes. A schematic of the field-effect-transistor configuration is shown in Figure 4b.[29] The $Si/SiO_2$ chip along with the electrodes and the graphene sheet are brought in contact with a droplet of water containing 10 mM KCl. A Ag/AgCl reference electrode also immersed in the droplet acts as the gate. The resistance of the graphene sheet across the source (S)−drain (D) electrodes (typical electrode spacing: 3−4 $\mu$m) is measured as a function of the voltage applied to the gate electrode, $V_G$. In this configuration, the electrical double layer at the graphene/liquid interface serves as the gate capacitor.[29] Figure 4c shows the measured resistance as a function of gate voltage, $V_G$, for both reference and peeled-off graphene devices. Several features immediately distinguish the transport characteristics of the two samples. The graphene synthesized on peeled-off Cu foil exhibits a narrow resistivity peak (fwhm is ~0.28 V), with the charge neutrality point (CNP) very close to zero ($V_G$ = 0.027 V). For reference graphene, the fwhm is 0.44 V and the CNP is 0.18 V. Furthermore, the

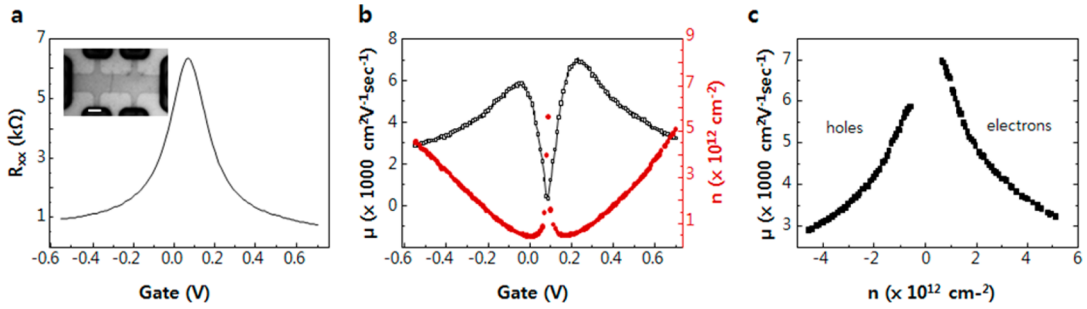


**Figure 5. Hall effect measurements on graphene devices. (a) 4-probe resistance of a (peeled-off) graphene Hall-bar as a function of the liquid gate voltage; the inset shows an optical image of the Hall bar (scale bar, 5 $\mu$m). (b) Mobility and charge carrier concentration as a function of the liquid gate voltage. (c) Mobility as a function of charge carrier concentration. Negative values on *X*-axis denote holes, while positive values denote electrons (see also Supporting Information Figure S6).**

peeled-off graphene exhibits low resistance. Charge carrier mobility is derived from a modified Drude model, which is fitted to the resistance measurements shown as the red curves in Figure 4c (see Supporting Information Figure S8).[30] The charge carrier mobility of peeled-off graphene was found to be as high as 29 000 $cm^2\ V^{-1}\ s^{-1}$. These features indicate a higher degree of order and reduced impurity doping in the peeled-off graphene. This may be partly due to the improved order of the catalyst surface. We used AFM to examine the catalyst surface after CVD growth. See Supporting Information Figure S9. The step-terrace structure of the peeled-off Cu surface shows parallel aligned steps. For normal Cu foil, the steps are rounded. This may mean that the step-terrace structure of peeled-off Cu offers an advantage to carrier mobility as nano-ripples[11] are expected to likewise be parallel aligned; hence mobility in certain directions may be improved. We note that this value approaches the upper limit of charge carrier mobility that can be obtained with this method. Similar mobility values were obtained on other samples, with values in the range of 8000–30 000 $cm^2\ V^{-1}\ s^{-1}$ for peeled-off graphene in comparison to 1500–10 000 $cm^2\ V^{-1}\ s^{-1}$ for reference graphene.

To gather further evidence of the high carrier mobility of the peeled-off graphene, we also performed Hall bar measurements in liquid. Figure 5 collects the 4-probe resistance, mobility and charge carrier concentration as a function of the applied gate voltage. It is apparent that for this sample, we observe a charge carrier mobility of around 6500 $cm^2\ V^{-1}\ s^{-1}$ at a carrier concentration of around $4.2 \times 10^{11}\ cm^{-2}$ (for both holes and electrons). Similar values in the range of 5000 to 10 000 $cm^2\ V^{-1}\ s^{-1}$ are obtained for other samples with the highest observed mobility of around 10 100 $cm^2\ V^{-1}\ s^{-1}$ at a carrier concentration of $4.7 \times 10^{11}\ cm^{-2}$ (see Supporting Information Figure S10). However, in these devices, the transport is asymmetric with electron mobilities much higher than that of holes.[31] The mobility values observed in the Hall measurements are lower than that of the field-effect mobilities. This may be attributed partly to the larger sizes of the structures here (length and width of central Hall bar is 10 $\mu$m × 5 $\mu$m) in comparison to the field-effect devices. It is also worth pointing out that the lowest carrier densities that we can attain using liquid gating are much higher than the concentration values typically reported for back-gated devices. Most likely, the presence of the liquid/ionic background along with the use of $SiO_2$ substrate limits the performance of our devices to these mobility values.[32]

## CONCLUSIONS

To summarize and conclude, we report a novel CVD graphene synthesis, which relies on a near perfect (111) copper surface catalyst produced by epitaxial growth on C-plane sapphire and a simple peel-off procedure. The "peeled-off" catalyst produces CVD graphene, which exhibits electronic performance comparable to that of exfoliated graphene, with domain sizes larger than 100 $\mu$m. The sapphire mother substrate can be used over and over to produce additional copper foil catalyst. As a result of progress in crystal growth technology, one can realistically speculate that this peel-off approach can be scaled to produce graphene sheets several tens of centimeters in size. This peeling off approach can certainly also be applied to a number of other catalytically important metal foils such as nickel, cobalt, iron, ruthenium, palladium, iridium, platinum, and their alloys. These results provide new opportunities for complementary technological advancements for high quality and large-area graphene devices.

## METHODS

**Preparation of Cu Foil.** C-plane sapphire (double side polished, Crystal Bank Research Institute in Pusan National University, Korea) was used as a mother substrate. After Cu films were cleaned sequentially with acetone, isopropyl alcohol, and deionized water, they were deposited by electron beam deposition using a high purity Cu source from Sigma-Aldrich (item number: 254177, Cu beads, 2–8 mm, 99.9995% trace metals basis). The sapphire substrate was dipped in HCl + DI (volume ratio 1:1) during 1–2 min to remove surface contamination right before Cu deposition. The Cu films were grown to 50 nm thickness at a rate of 0.03 nm/c. The growth chamber pressure was

maintained at about $10^{-6}$ Torr during deposition, and the substrate was held at room temperature. For the Cu plating on epitaxial Cu film, the cathode (50 nm Cu film on C-plane sapphire) and anode (Bulk Cu stick) were electrically connected with a Keithley 2400 digital source meter for the constant current density (15 mA/cm$^2$). During electroplating, the voltage between electrodes varied between 0.2 and 0.3 V and the growth rate was about 16 $\mu$m/h and controlled to yield a final thickness of $\sim$25 $\mu$m. The temperature of the electroplating solution was 60 °C. Due to large compressive stress between the thick Cu foil and the C-plane sapphire substrate, all Cu foils could easily be peeled-off from the sapphire substrate.

**Graphene Growth.** The peeled-off Cu foils were loaded into a quartz tube reaction chamber. A growth process is as follows. First, the pressure in the growth chamber is pumped down to 3 mTorr using a mechanical pump. Second, a 40 sccm flow of hydrogen gas is introduced into the chamber at 950 mTorr. Third, the Cu foils were heated to 1000 °C over 60 min. Fourth, 6 sccm flow of methane gas with 20 sccm hydrogen is introduced into the chamber for 10 min with a total pressure of 460 mTorr for graphene synthesis; after growth, the furnace was cooled down rapidly to room temperature under a 20 sccm flow of hydrogen.

For the reference graphene on normal Cu foil (Alfa Aesar, item No. 13382, 99.8% purity), the Cu foils were first immersed in 0.3 mol ammonium persulfate ($(NH_4)_2S_2O_8$, Sigma-Aldrich, item No. 248614, ACS reagent, $\geq$98.0%) solution for 1 min and then loaded into the quartz tube reaction chamber. We used $(NH_4)_2S_2O_8$ for the Cu etching; it is advantageous to use etching solutions that are free from contamination by iron containing compounds, such as $Fe(NO_3)_3$ and $FeCl_3$ solutions. A typical growth process for the reference graphene is same except the third step where the additional 30 min annealing is needed to enlarge the Cu grains

**Graphene Transfer.** To transfer the graphene samples, first, one side of the graphene/Cu foils was spin coated with poly(methyl methacrylate) (PMMA) on a spin coater at 2000 rpm for 60 s and dried in atmosphere for 1 h. Then, the uncoated side of the graphene samples, that is, the side that is polymer free, was etched in an oxygen plasma for 30 s at 100 W to remove Carbon. After the Cu foils were totally etched away in $(NH_4)_2S_2O_8$ solution (0.3 M) for 12 h, the floating graphene/PMMA films were washed in several cycles with DI water. The resulting graphene/PMMA films were transferred onto a target substrate and dried at ambient conditions for 24 h before being heat treated at 180 °C for 30 min to increase the adhesion between graphene and target substrate ($SiO_2$ covered Si substrate or TEM Cu-grid). Then, the PMMA layers were finally removed sequentially by washing with acetone, isopropyl alcohol, and deionized water.

**Characterization of Samples.** High-resolution X-ray diffraction (XRD) using synchrotron radiation was performed at the 3D beamline at Pohang Accelerator Laboratory (PAL). The atomic force microscopy (AFM) images were recorded using a Digital Instruments Nanoscope in tapping mode using silicon cantilevers. The 3D profiling was carried out using a Wyko-NT1100 from Veeco. X-ray photoemission spectra (XPS) were obtained at the 8A1 beamline at the PAL. Liquid crystals from Sigma-Aldrich (item number: 328510, 4′-pentyl-4-biphenylcarbonitrile liquid crystal (nematic), 98%) were directly spin-coated onto the graphene surface at 2000 rpm. Below the isotropic transition temperature of liquid cystal (40 °C), we can see the grain distribution of graphene using polarized light in conventional optical microscope by checking the distribution of the liquid crystal on graphene. The transmission electron microscopy (TEM) images were collected using a Philips CM12 instrument with a $LaB_6$ filament operated at an electron energy of 80 keV. The Raman spectra were obtained with a LabRAM HR 800 (HORIBA Yvon GmbH) spectrometer under the following conditions: excitation wavelength of the laser, He−Ne 633 nm; spot size of the laser beam, 5 $\mu$m in diameter; measurement time, 20 s. Surface investigations were performed with a scanning electron microscope (SEM) Leo 1525 equipped with an electron backscatter diffraction (EBSD) system. The Hall bar measurements are carried out also in liquid. The 4-probe resistance ($R_{xx}$) and the magnetoresistance ($R_{xy}$) are measured using a permanent magnet (0.3 T) for three different magnetic fields (0, $+B$, $-B$) at every gate voltage. The carrier concentration and the mobility as a function of applied gate voltage are extracted subsequently from these measurements.

*Conflict of Interest:* The authors declare no competing financial interest.

*Acknowledgment.* A.M.W. acknowledges the Alexander von Humboldt Foundation for support in the form of an Alexander Humboldt Professorship. M.M. and C.R. acknowledge funding by the Deutsche Forschungsgemeinschaft (ZuK 45-1). We thank Bonhyeong Koo in POSTECH for assistance in optimizing the Cu plating and measuring the XRD, and Dr. Sascha Schäfer (University of Göttingen) for optimizing nematic liquid crystal (4-pentyl-4′-cyanobiphenyl (5CB)) coating and polarized optical microscopy. We thank Stephan Schmid and Yvonne Link for metal evaporation for graphene devices.

*Supporting Information Available:* (1) Domain mismatch in Cu/C−$Al_2O_3$ system, (2) EBSD of Cu foils, (3) O 1s XPS spectra of Cu foils, (4) graphene growth on epitaxial Cu (111)/C-sapphire without plating and peeling off, (5) prereduction of normal Cu foil-removal of native oxide by acetic acid, (6) prereduction of normal Cu foil-removal of native oxide by ammonium persulfate, (7) EBSD results of peeled-off Cu foil after graphene growth, (8) high carrier mobility derived from Drude model fit to field effect measurements, (9) step-terrace of Cu foils after graphene growth, (10) high carrier mobility derived from Hall bar measurements. This material is available free of charge *via* the Internet at http://pubs.acs.org.

## REFERENCES AND NOTES

1. Li, X. S.; Cai, W. W.; An, J. H.; Kim, S.; Nah, J.; Yang, D. X.; Piner, R.; Velamakanni, A.; Jung, I.; Tutuc, E.; *et al.* Large-Area Synthesis of High-Quality and Uniform Graphene Films on Copper Foils. *Science* **2009**, *324*, 1312–1314.
2. Bae, S.; Kim, H.; Lee, Y.; Xu, X. F.; Park, J. S.; Zheng, Y.; Balakrishnan, J.; Lei, T.; Kim, H. R.; Song, Y. I.; *et al.* Roll-to-Roll Production of 30-Inch Graphene Films for Transparent Electrodes. *Nat. Nanotechnol.* **2010**, *5*, 574–578.
3. Novoselov, K. S.; Fal'ko, V. I.; Colombo, L.; Gellert, P. R.; Schwab, M. G.; Kim, K. A. Roadmap for Graphene. *Nature* **2012**, *490*, 192–200.
4. Kim, K. S.; Zhao, Y.; Jang, H.; Lee, S. Y.; Kim, J. M.; Kim, K. S.; Ahn, J.-H.; Kim, P.; Choi, J.-Y.; Hong, B. H. Large-Scale Pattern Growth of Graphene Films for Stretchable Transparent Electrodes. *Nature* **2009**, *457*, 706–710.
5. Geim, A. K. Graphene: Status and Prospects. *Science* **2009**, *324*, 1530–1534.
6. Wood, J. D.; Schmucker, S. W.; Lyons, A. S.; Pop, E.; Lyding, J. W. Effects of Polycrystalline Cu Substrate on Graphene Growth by Chemical Vapor Deposition. *Nano Lett.* **2011**, *11*, 4547–4554.
7. Hu, B.; Ago, H.; Ito, Y.; Kawahara, K.; Tsuji, M.; Magome, E.; Sumitani, K.; Mizuta, N.; Ikeda, K.-i.; Mizuno, S. Epitaxial Growth of Large-Area Single-Layer Graphene over Cu(111)/Sapphire by Atmospheric Pressure CVD. *Carbon* **2012**, *50*, 57–65.
8. Gao, L.; Guest, J. R.; Guisinger, N. P. Epitaxial Graphene on Cu(111). *Nano Lett.* **2010**, *10*, 3512–3516.
9. Han, G. H.; Guenes, F.; Bae, J. J.; Kim, E. S.; Chae, S. J.; Shin, H.-J.; Choi, J.-Y.; Pribat, D.; Lee, Y. H. Influence of Copper Morphology in Forming Nucleation Seeds for Graphene Growth. *Nano Lett.* **2011**, *11*, 4144–4148.
10. Song, H. S.; Li, S. L.; Miyazaki, H.; Sato, S.; Hayashi, K.; Yamada, A.; Yokoyama, N.; Tsukagoshi, K. Origin of the Relatively Low Transport Mobility of Graphene Grown through Chemical Vapor Deposition. *Sci. Rep.* **2012**, *2*, 337.
11. Ni, G.-X.; Zheng, Y.; Bae, S.; Kim, H. R.; Pachoud, A.; Kim, Y. S.; Tan, C.-L.; Im, D.; Ahn, J.-H.; Hong, B. H.; *et al.* Quasi-Periodic Nanoripples in Graphene Grown by Chemical Vapor Deposition and Its Impact on Charge Transport. *ACS Nano* **2012**, *6*, 1158–1164.

12. Reddy, K. M.; Gledhill, A. D.; Chen, C.-H.; Drexler, J. M.; Padture, N. P. High Quality, Transferrable Graphene Grown on Single Crystal Cu(111) Thin Films on Basal-Plane Sapphire. *Appl. Phys. Lett.* **2011**, *98*, 113117.
13. Orofeo, C. M.; Hibino, H.; Kawahara, K.; Ogawa, Y.; Tsuji, M.; Ikeda, K.-i.; Mizuno, S.; Ago, H. Influence of Cu Metal on the Domain Structure and Carrier Mobility in Single-Layer Graphene. *Carbon* **2012**, *50*, 2189–2196.
14. Miller, D. L.; Keller, M. W.; Shaw, J. M.; Chiaramonti, A. N.; Keller, R. R. Epitaxial (111) Films of Cu, Ni, and $Cu_xNi_y$ on Alpha-$Al_2O_3$ (0001) for Graphene Growth by Chemical Vapor Deposition. *J. Appl. Phys.* **2012**, *112*, 064317.
15. Khattak, C. P.; Guggenheim, P. J.; Schmid, F. Growth of 15-Inch Diameter Sapphire Boules. In *Window and Dome Technologies VIII*; Tustison, R. W., Ed.; SPIE: Bellingham, WA, 2003; Vol. 5078, pp 47–53.
16. Khattak, C. P.; Schmid, F. Growth of the World's Largest Sapphire Crystals. *J. Cryst. Growth* **2001**, *225*, 572–579.
17. Schmid, F.; Khattak, C. P.; Felt, D. M. Producing Large Sapphire for Optical Applications. *Am. Ceram. Soc. Bull.* **1994**, *73*, 39–44.
18. Oh, S. H.; Scheu, C.; Wagner, T.; Ruehle, M. Control of Bonding and Epitaxy at Copper/Sapphire Interface. *Appl. Phys. Lett.* **2007**, *91*, 141912.
19. Yu, H. K.; Baik, J. M.; Lee, J.-L. Self-Connected and Habitually Tilted Piezoelectric Nanorod Array. *ACS Nano* **2011**, *5*, 8828–8833.
20. Yu, H. K.; Baik, J. M.; Lee, J.-L. Design of an Interfacial Layer to Block Chemical Reaction for Epitaxial ZnO Growth on a Si Substrate. *Cryst. Growth Des.* **2011**, *11*, 2438–2443.
21. Chavez, K. L.; Hess, D. W. A Novel Method of Etching Copper Oxide Using Acetic Acid. *J. Electrochem. Soc.* **2001**, *148*, G640–G643.
22. Biesinger, M. C.; Lau, L. W. M.; Gerson, A. R.; Smart, R. S. C. Resolving Surface Chemical States in XPS Analysis of First Row Transition Metals, Oxides and Hydroxides: Sc, Ti, V, Cu and Zn. *Appl. Surf. Sci.* **2010**, *257*, 887–898.
23. Levendorf, M. P.; Ruiz-Vargas, C. S.; Garg, S.; Park, J. Transfer-Free Batch Fabrication of Single Layer Graphene Transistors. *Nano Lett.* **2009**, *9*, 4479–4483.
24. Zhang, B.; Lee, W. H.; Piner, R.; Kholmanov, I.; Wu, Y.; Li, H.; Ji, H.; Ruoff, R. S. Low-Temperature Chemical Vapor Deposition Growth of Graphene from Toluene on Electropolished Copper Foils. *ACS Nano* **2012**, *6*, 2471–2476.
25. Luo, Z.; Lu, Y.; Singer, D. W.; Berck, M. E.; Somers, L. A.; Goldsmith, B. R.; Johnson, A. T. C. Effect of Substrate Roughness and Feedstock Concentration on Growth of Wafer-Scale Graphene at Atmospheric Pressure. *Chem. Mater.* **2011**, *23*, 1441–1447.
26. Kim, D. W.; Kim, Y. H.; Jeong, H. S.; Jung, H.-T. Direct Visualization of Large-Area Graphene Domains and Boundaries by Optical Birefringency. *Nat. Nanotechnol.* **2012**, *7*, 29–34.
27. Hao, Y. F.; Bharathi, M. S.; Wang, L.; Liu, Y. Y.; Chen, H.; Nie, S.; Wang, X. H.; Chou, H.; Tan, C.; Fallahazad, B.; *et al.* The Role of Surface Oxygen in the Growth of Large Single-Crystal Graphene on Copper. *Science* **2013**, *342*, 720–723.
28. Malard, L. M.; Pimenta, M. A.; Dresselhaus, G.; Dresselhaus, M. S. Raman Spectroscopy in Graphene. *Phys. Rep.* **2009**, *473*, 51–87.
29. Chen, F.; Qing, Q.; Xia, J.; Li, J.; Tao, N. Electrochemical Gate-Controlled Charge Transport in Graphene in Ionic Liquid and Aqueous Solution. *J. Am. Chem. Soc.* **2009**, *131*, 9908–9909.
30. Kim, S.; Nah, J.; Jo, I.; Shahrjerdi, D.; Colombo, L.; Yao, Z.; Tutuc, E.; Banerjee, S. K. Realization of a High Mobility Dual-Gated Graphene Field-Effect Transistor with $Al_2O_3$ Dielectric. *Appl. Phys. Lett.* **2009**, *94*, 062107.
31. Bolotin, K. I.; Sikes, K. J.; Jiang, Z.; Klima, M.; Fudenberg, G.; Hone, J.; Kim, P.; Stormer, H. L. Ultrahigh Electron Mobility in Suspended Graphene. *Solid State Commun.* **2008**, *146*, 351–355.
32. Chen, J.-H.; Jang, C.; Xiao, S.; Ishigami, M.; Fuhrer, M. S. Intrinsic and Extrinsic Performance Limits of Graphene Devices on $SiO_2$. *Nat. Nanotechnol.* **2008**, *3*, 206–209.